ACTA SCIENTIARUM POLONORUM
Acta Sci. Pol. Hortorum Cultus, 19(3) 2020, 111–124
https://czasopisma.up.lublin.pl/index.php/asphc ISSN 1644-0692 e-ISSN 2545-1405 DOI: 10.24326/asphc.2020.3.10
ORIGINAL PAPER
Accepted: 25.07.2019

MOLECULAR CLONING, BIOINFORMATION ANALYSIS AND EXPRESSION OF THE STRICTOSIDINE SYNTHASE IN *Dendrobium officinale*

Yan-Fang Zhu[1,2] ✉, Hong-Hong Fan[2], Da-Hui Li[2], Qing Jin[2], Chuan-Ming Zhang[2], Li-Qin Zhu[2], Cheng Song[2], Yong-Ping Cai[2], Yi Lin[2]

[1] Key Laboratory of Resource Plant Biology of Anhui Province, School of Life Sciences, Huaibei Normal University, Huaibei 235000, P.R. China

[2] School of Life Sciences, Anhui Agricultural University, Hefei, 230036, P.R. China

ABSTRACT

The enzyme strictosidine synthase (STR, EC: 4.3.3.2) plays a key role in the biosynthetic pathway of terpenoid indole alkaloid (TIA). It catalyzes the condensation of the tryptamine and secologanin to form 3α(S)-strictosidine, which is the common precursor of all TIAs. In this paper, a *STR* gene designated as *DoSTR* (GenBank: KX068707) was first cloned and characterized from *Dendrobium officinale* with rapid amplified cDNA ends method (RACE). *DoSTR* has a length of 1380bp with 1179bp open reading frame encoding 392 amino acids. BlastP analyses showed that its amino acid sequence was classified into Str_synth superfamily. qRT-PCR showed that *DoSTR* was expressed in all tissues tested, with a significantly higher level in flower and the lowest in stem. Four different treatments with MeJA, SA, ABA and $AgNO_3$, respectively, could induce the *DoSTR* expression to a different extent. And the effect of MeJA was the most obvious and transcript level of *DoSTR* induced by MeJA was 20.7 times greater than that of control at 48 hours after treatment. Furthermore, it was found that *DoSTR* was localized in vacuole through transient expression in tobacco. The characterization and expression of *DoSTR* can help in further studying the role of DoSTR in the biosynthesis of TIAs in *D. officinale.* This study may throw light on the alkaloid biosynthesis pathway of *D. officinale*.

Key words: *Dendrobium officinale*, *DoSTR*, terpenoid indole alkaloid, tissue expression pattern, subcellular localization

Abbreviations: TIA – terpenoid indole alkaloid, RACE – rapid amplification of cDNA ends, ORF – open reading fram, MeJA – methyljasmonate, SA – salicylic acid, ABA – absdcisic acid, $AgNO_3$ – silver nitrate, STR – strictosidine synthase, CAT – camptothecin, qRT-PCR Real-time quantitative PCR

INTRODUCTION

Dendrobium officinale Kimura et Migo is a renowned *Dendrobium* genus medicinal plant in traditional Chinese medicine. It has been widely used in China owing to its diverse tonic components. The main active ingredients of *D. officinale* include polysaccharides, alkaloids, phenols, coumarins, terpenes, flavonoids, amino acids, benzyl compounds, and some trace mineral elements [Ng et al. 2012, Xu et al. 2013]. Due to these components, *D. officinale* possesses immunomodulatory and hepatoprotective activities,

✉ yfangok@163.com

antioxidant, anticancer, neuroprotective activities, anti-cataract, and so on [Ng et al. 2012, Wei et al. 2016]. Among these medicinal ingredients, although alkaloids are one of the most important components of *D. officinale*, the biosynthesis pathway of these alkaloids is still unclear.

In a previous report, the alkaloids of *Dendrobium* genus are mostly sesquiterpene alkaloids [Zhang et al. 2003]. Based on the *D. officinale* genome data and metabolic profiling, the pathway of *D. officinale* alkaloid synthesis could be extended to generate a kind of terpenoid indole alkaloid (TIA) [Yan et al. 2015, Jiao et al. 2018]. Moreover, according to the published *D. officinale* transcriptome data, genes annotated as elements of *D. officinale* alkaloid biosynthetic pathways were enriched in the TIA biosynthesis pathway [Guo et al. 2013].

TIA is a large group of secondary metabolites in plants with many pharmaceutical effects, such as camptothecin, vinblastine and vincristine exhibiting excellent anti-tumor activities [Mcknight et al. 1991, Venditto et al. 2010], ajmalicine and serpentine being used in the treatment of cardiac and circulatory [Pasquali et al. 1992], raubasine and reserpine treating hypertension, high dosage of reserpine curing schizophrenia [Ma 2006]. All of TIAs are derived from the common precursor 3α (S) -strictosidine, which is catalyzed by strictosidine synthase (STR, EC: 4.3.3.2) [Pasquali et al. 1992, Yamazaki et al. 2003]. Thus, the STR is considered as a key enzyme in TIA biosynthesis [Cui et al. 2015, Lu et al. 2009, Wungsintaweekul et al. 2012].

Although STR plays a key role in the TIAs biosynthesis, its sequence and characteristics in *D. officinale* are unknown. In this study, *STR* was cloned from *D. officinale* for the first time. Its bioinformation, tissue-specific expression, regulation by different phytohormones, subcellular localization were investigated. These researches are important for the biosynthesis of alkaloid in *D. officinale*.

MATERIALS AND METHODS

Plant materials. Two years old *D. officinale* wild plants which were grown in 20 cm height and 25 cm inner dimeter round plastic pots filled with a substrate mix of small pine bark and sand, were identified by Professor Cai Yongping of Anhui Agricultural University and used as the experimental materials which grew in wild environment and obtained from Dabie Mountain Area in Huoshan county, Anhui province, China. The current-year leaves were immediately frozen in liquid nitrogen and stored at –80°C, which were used to extract RNA for cloning *DoSTR* putative gene sequence.

For further analysis *DoSTR* expression in different tissues (roots, stems, flowers and leaves), 0.5 grams of each tissue were collected from the above described plants, quickly frozen and stored at –80°C, respectively. Protocorms were induced from seeds on MS medium by the tissue culture. After cultured with temperature 25/25°C (day/night) under darkness for 30 days. Then, it was transferred on MS medium supplemented with 1.0 mg L^{-1} 6-BA, 0.1 mg L^{-1} NAA and 30 g L^{-1} sucrose. By liquid suspension culture with temperature 25/25°C (day/night) under darkness for 60 days, uniform size protocorms were collected for RNA extraction.

In order to analysis the *DoSTR* response to different stresses, some phytohormones were used to simulated stresses. And protocorms were cultivated on MS medium supplemented with 100 μmol L^{-1} methyljasmonate (MeJA), 100 μmol L^{-1} salicylic acid (SA), 100 μmol L^{-1} absdcisic acid (ABA) and 30 μmol L^{-1} silver nitrate ($AgNO_3$), respectively. The protocorms treated by MeJA and SA were collected at 0, 2, 4, 8, 24, 48, 72 h and prepared for gene's expression analysis, while those treated by ABA and $AgNO_3$ were collected at 0, 1, 2, 3, 4, 7 d, respectively. Untreated protocorms were collected at different time as control.

RNA extraction and cDNA synthesis. Total RNAs from five different organs were isolated with RNAprep Pure Plant Kit (Tiangen, China) using about 0.5 g tissue grinded in liquid nitrogen. The quality and concentration of RNA were measured by NanoDrop 2000 (Thermo). High quality RNA was used for the reverse transcription. The 3'- and 5'-RACE-Ready cDNA were reverse transcribed from the leaf total RNA using the SMARTer® RACE 5'/3'Kit (Clontech, US), according to the manufacturer's instruction. First-strand cDNA for qRT-PCR was reverse transcribed from total RNAs using the PrimeScript RT Reagent Kit with gDNA Eraser (DDR047A, Takara, China).

Cloning and sequencing the full-length cDNA of *DoSTR*. To obtain the full-length cDNA sequence of

DoSTR from *D. officinale*, 5'- and 3'-RACE experiments were carried out according to the SMARTer® RACE 5'/3'Kit user's manual. The gene-specific primers EST-F and EST-R and the 3'RACE and 5'RACE nested primers were shown in the Table 1.

Amplified fragments of 5'- and 3'-RACE were purified and cloned into the pMD18-T vector (Takara, China), transformed into *E. coli* DH5α cells, and then cultured in LB medium at 37°C in the dark for sequencing. The complete sequence was assembled using DNAMAN software into a full-length *DoSTR* cDNA sequence. Primers to amply the full-length cDNA (Tab. 1) were designed based on the assembled core fragments of the 5'-and 3'-RACE sequences, and then to PCR and sequence.

Tab. 1. Names and sequences of primers

	Primers name	Sequences (5'–3')
STR-EST	EST-F	GCTTGAACTGCTGGAGGAT
	EST-R	ACGGCTATGAATGACATTAAGACA
3'RACE	3'-OUT	TTTCACTGCTGAGCCTTCTGGGA
	3'-IN	CAATGAAGGCAATCGTGGAAGG
5'RACE	5'-OUT	GCCTTGTCACCTTTCAGCCAGTATC
	5'-IN	AAGGTCTCGCAAGAGGACAGTGGTT
Full-length cDNA	STR-F	ATGGCACTCGCTGGGGCT
	STR-R	TTACTCTAATGTAAATACGGCTATGAATGG
18SrRNA	F	GAGCGAACAGGATTAGATACCC
	R	TCCTTTGAGTTTCGGTCTTGCG
DoSRT subcellular localization	F	CGGGGTACCATGGCACTCGCTG
	R	CGCGGATCCCTCTAATGTAAATACGGCTA

Sequences with underline are primers with restriction site

Sequence analysis of *DoSTR*. The ORF of *DoSTR* was deduced using the online tool ORF Finder and ORF Finder is a widely used resource in National Center for Biotechnology Information (NCBI) [http://www.ncbi.nlm.nih.gov/orffinder/, Wheeler et al. 2007]. The theoretical isoelectric point (pI) and molecular mass for the protein were predicted by using the ExPASyProtParam tool and ExPASy [http://www.expasy.org] has worldwide reputation as one of the main bioinformatics resources for proteomics [Artimo et al. 2012]. The protein subcellular localization and secondary structure were predicted by PredictProtein and PredicProtein is an open resource for online prediction of protein structural and functional features [https://www.predictprotein.org/, Yachdav et al. 2014]. N-signal peptides were predicted using SignalP 5.0 which can predict the presence of signal peptides and the location of their cleavage sites in protein from biology [http://www.cbs.dtu.dk/services/SignalP/, Almagro Armenteros et al. 2019]. The structural model of DoSTR was built by homology modeling based on crystal structure of homologous in SWISS-MODEL. The deduced amino acid sequences were aligned with DNAMAN and used to construct a neighbor-joining tree in MEGA5 with default settings at least 1000 bootstrap replicates.

***DoSTR* relative expression analysis.** To compare tissue-specific expression profiles of *DoSTR*, transcripts of five organs were assayed. And for further analysis of the response of *DoSTR*, MeJA, SA and ABA three plant growth substances and $AgNO_3$ were used to treat protocorms, respectively. 0.5 grams protocorms of different treatment time were collected and investigated. qRT-PCR was performed using a SYBR

Premix Ex Taq™ II (Takara, China) and detected by a CFX96 Real-Time system (BIO RAD, US). The relative expression value was calculated using the $2^{-\Delta\Delta Ct}$ method [Pfaffl 2001], with *D. officinale* 18SrRNA as an internal control. And reactions were performed in triplicate.

***DoSTR* transient expression and subcellular localization.** To analyze *DoSTR* transient expression, we used a pCambia1301-eGFP expression vector. Primers with restriction site were designed to amplify the *DoSTR* ORF region from cDNA (Tab. 1). The PCR products were separated and purified. The purified DNA and empty expression vector pCambia1301-eGFP were cleaved with KpnI and BamHI, respectively, and then separated and purified. The two purified products were fused and linked by T4 ligase (Takara, China). Then the recombinant vectors were transformed into *E. coli* DH5α, and individual clones were selected to obtain positive recombinants as confirmed by sequencing. The recombinant vector was named as pCambia1301-DoSTR-eGFP. The empty expression vector pCambia1301-eGFP served as a negative control. Then the constructed vectors were transformed into *Agrobacterium tumefaciens* EHA105 with electroporation. And the suspensions of *A. tumefaciens* EHA105 were injected into the leaves of tobacco (*N. tabacum*). After culturing in the dark 48 h, the leaves of tobacco were zoomed in a confocal laser scanning microscope (Olympus, Japan).

RESULTS

Cloning and characterization of *DoSTR*. Based on the previous transcriptome analysis of *D. officinale*, the expressed sequence tags (EST) of *DoSTR* was obtained [Guo et al. 2013]. Using the special primers designed by the EST, 5'RACE and 3'RACE of *DoSTR* were performed (Fig. 1). Two cDNA fragments of 801 bp and 529 bp were sequenced. The full-length 1380 bp cDNA sequence of *DoSTR* was finally obtained from *D. officinale* by RACE method. There were a 96-bp 5'-untranslanted region (UTR) and a 105-bp 3'-UTR. BlastP analysis revealed that the sequence of this protein contained the conserved domain of strictosidine synthase and was classified into Str_synth superfamily. The results indicate that the gene is a member of the *STR* superfamily. Therefore, this gene was designated as *DoSTR* (GenBank accession number KX068707). As show in Figure 2, *DoSTR* cDNA contained a 1179 bp ORF encoding a 392-amino acid protein. The deduced protein had an isoelectric point (pI) of 7.64 and a calculated molecular mass of about 44.0 kD.

Bioinformatics analysis of DoSTR. Both the subcellular localization and secondary structure of DoSTR were predicted using the online tool PredictProtein [https://www.predictprotein.org/, Yachdav et al. 2014]. The predicted results showed that DoSTR was localized in the vacuole, and its secondary structure was

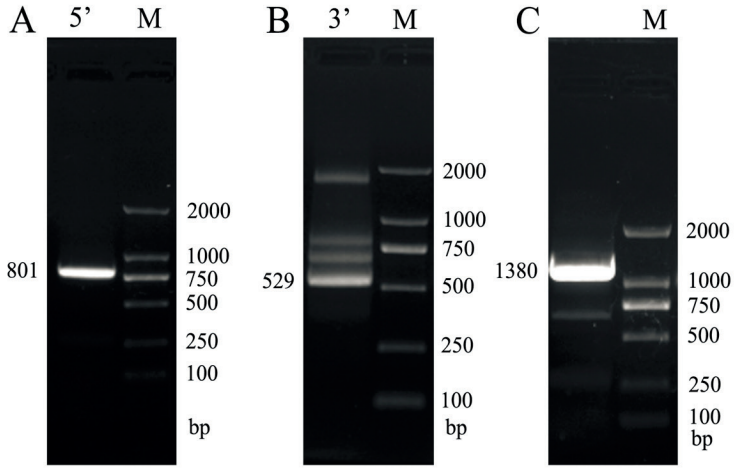

Fig. 1. Agarose gel electrophoresis of PCR products. A: the product of 5'RACE, B: the product of 3'RACE, C: full length of DoSTR

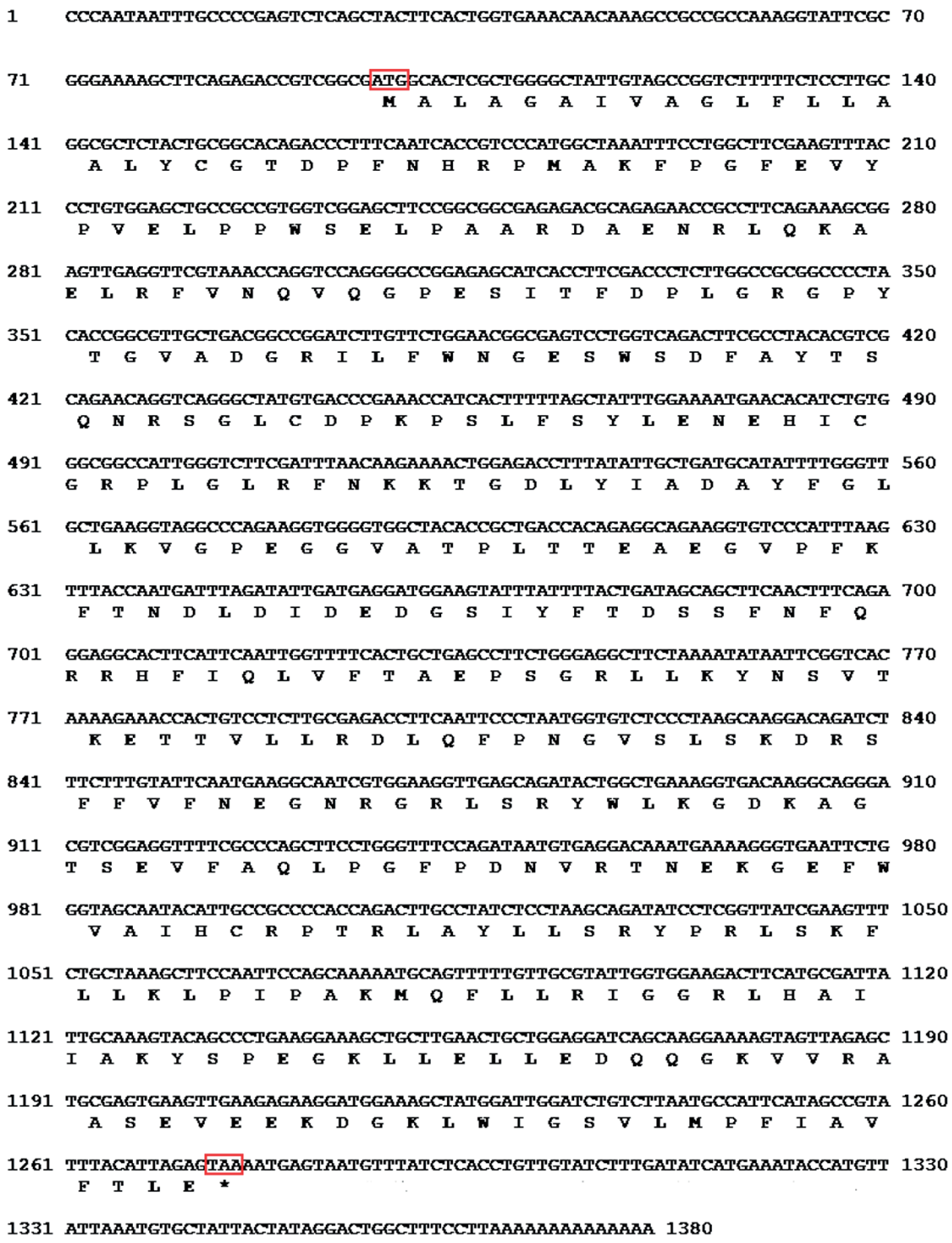

Fig. 2. The full length of *DoSTR* and its amino acid sequence. The start codon (ATG) and stop codon (TAA) were marked with box; M: DL 2000 marker

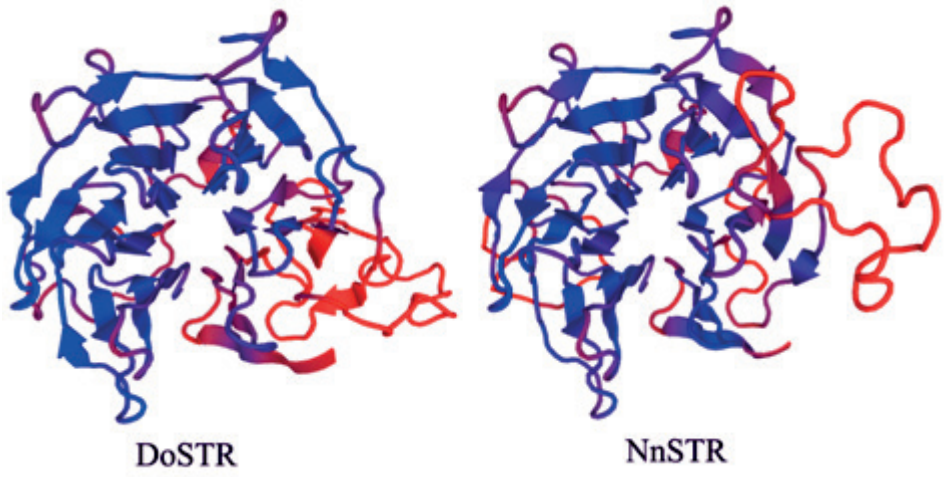

Fig. 3. The 3D structure of DoSTR and *Nothapodytes nimmoniana* STR established by homology-based modeling using the crystal structure of *Rauvolfia serpentina* STR as template

composed of 6.63% helix, 26.28% strand and 67.09% loop, indicating that DoSTR can be classified as a mixed protein.

According to N-signal peptide prediction, the amino acid sequence of DoSTR had a N-signal peptide with 23 residues, suggesting that it should function as a type of secretory protein.

The 3-dimensional structure of DoSTR protein was predicted by SWISS-MODEL based on crystal structure of homology, with the *Rauvolfia serpentina STR* protein structure as the template. The predicted structural model of DoSTR (without its N-signal peptide) was a kind of six-bladed β-propeller fold (Fig. 3), very similar to the 3D structure of *R. serpentina* STR [Ma 2006]. Their structural similarity suggests that they may share similar functions.

Multiple sequences alignment of DoSTR with other homologous STRs revealed that there existed a comparatively higher conservation (over 51% of identity) among various species (Fig. 4).

The constructed phylogenetic tree of multiple STRs from different plants showed that *D. officinale* STR was clustered together with STRs from *Zea mays* and *Elaeis guineensis*, two monocotyledon plants (Fig. 5). *Ophiorrhiza pumila* and *Mitragyna speciose* STRs from family Rubiaceae were clustered into one clade, while those of *Catharanthus roseus*, *Rauvolfia verticillata* and *Rauvolfia serpentine* from family Apocynaceae were included in a small group. The catalytic function of these STRs has been experimentally proved [Chen et al. 2008, Kutchan 1989, Mcknight et al. 1990]. Then two clades composed of STRs from Rubiaceae and Apocynaceae were further clustered together, both of which belong to the order Gentianales that has a variety of TIA secondary metabolites and active STRs. The phylogenetic relationship of DoSTR is in accordance with the traditional evolutionary classification of plants.

Additionally, although *Nothapodytes nimmoniana* from family Icacinaceae and order Celastrales, contains camptothecin, a kind of monoterpenoid indole alkaloid component [Manjunatha et al. 2016], its STR did not cluster with those of five species from order Gentianales. The STR of *N. nimmoniana* was firstly clustered with that of *Papaver somniferum*, then with 3 species of monocotyledon plants *D. officinale*, *Z. mays* and *E. guineensis*. The result showed that DoSTR was distant in evolution with the STRs from orders Gentianales, instead it was closely related with that of *N. nimmoniana*. When the two STR protein sequences of *D. officinale* and *N. nimmoniana* were aligned, it was found that they had a similarity value of 75% (Fig. 6).

Expression pattern of *DoSTR* in different tissues. To determine the tissue-specific expression of *DoSTR* patterns qRT-PCR experiment was performed. *DoSTR*

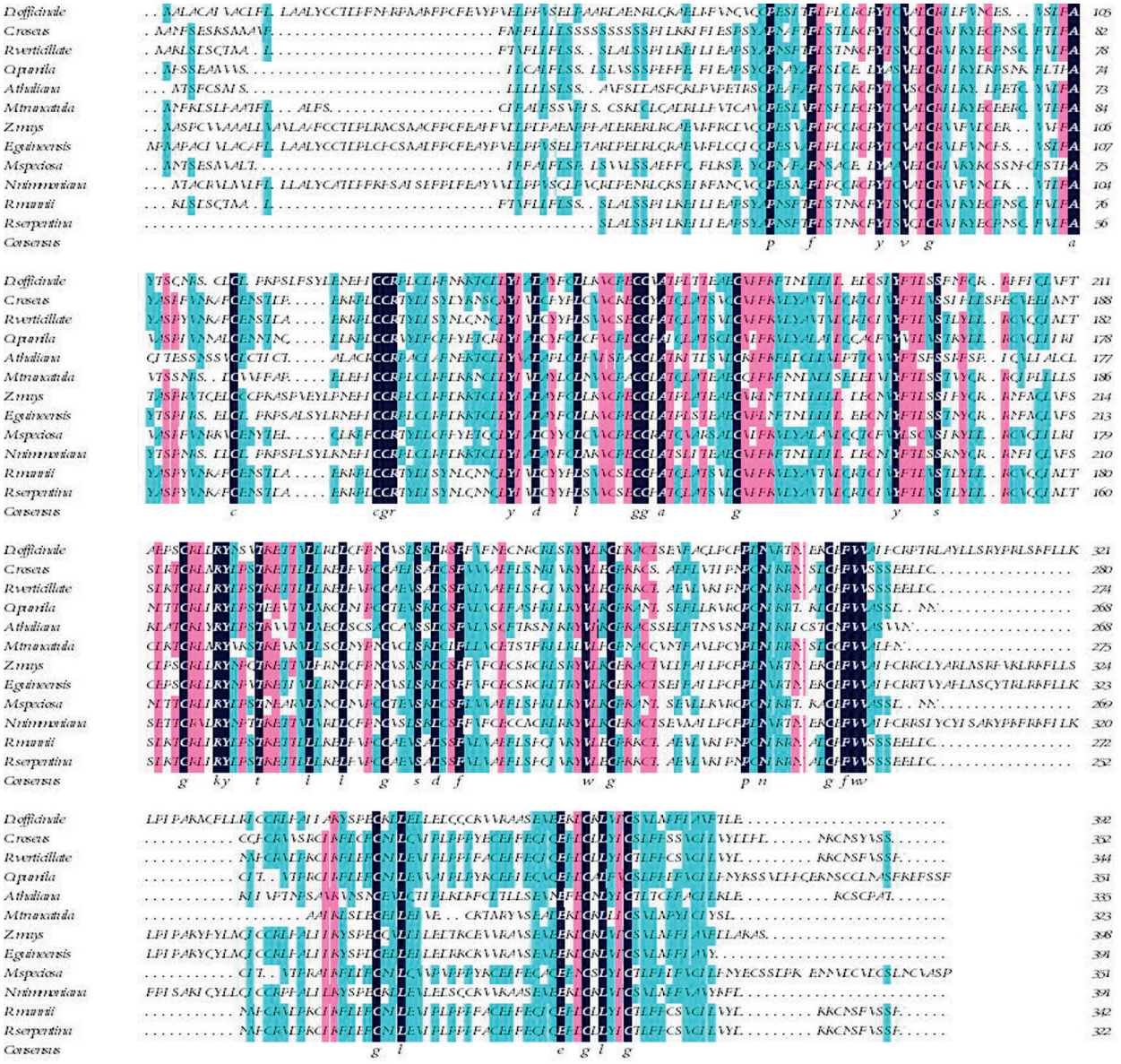

The black and colour boxes indicate the completely identical residues and the conserved residues among the aligned sequences, respectively. The amino acids residues pointed by red arrow are Cys-89, Cys-101 and Glu-309, respectively. STR protein sequences including *Z. mays* (*Zea mays* STR, NP_001150008.1), *A. thaliana* (*Arabidopsis thaliana* STR, NP_177542.1), *C. roseus* (*Catharanthus roseus* STR, CAA43936.1), *E. guineensis* (*Elaeis guineensis* STR, XP_010932965.1), *M. speciosa* (*Mitragyna speciosa* STR, ADK91432.1), *M. truncalula* (*Medicago truncatula* STR, XP_003617474.1), *O. pumila* (*Ophiorrhiza pumila* STR, BAB47180.1), *N. nimmoniana* (*Nothapodytes nimmoniana* STR, AIL49060.1), *R. mannii* (*Rauvolfia mannii* STR, P68174.1), *R. serpentine* (*Rauvolfia serpentine* STR, 2FP8), *R. verticillata* (*Rauvolfia verticillata* STR, AAY81922.1)

Fig. 4. Multiple sequence alignments of DoSTR with other known STR

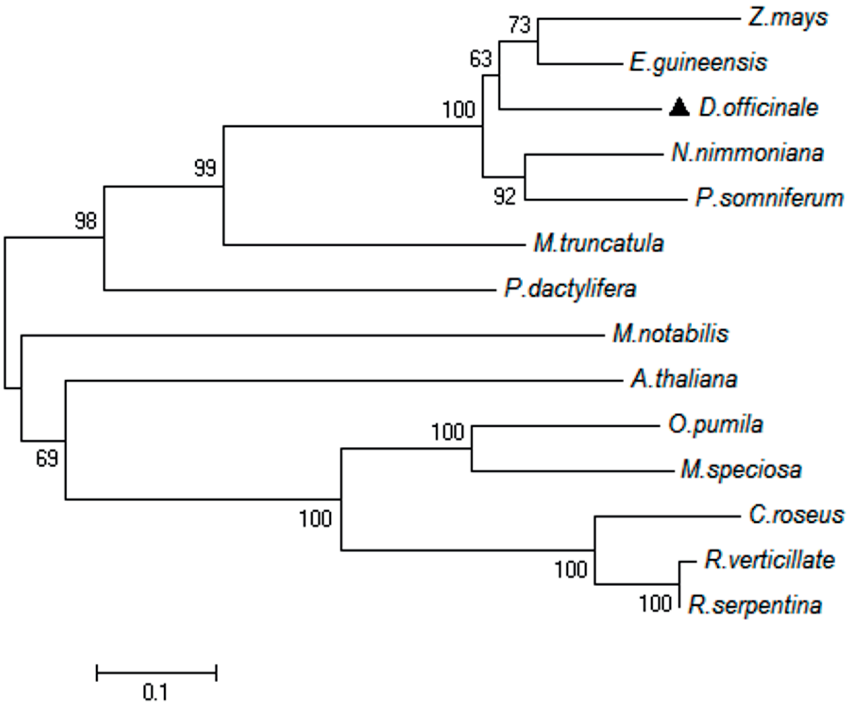

STR sequences from *Z. mays* (NP_001150008.1), *E. guineensis* (XP_010932965.1),*A. thaliana* (NP_177542.1), *C. roseus* (CAA43936.1), *M. notabilis* (XP_010110081.1), *M. truncatula* (XP_003617474.1), *O. pumila* (BAB47180.1), *P. dactylifera* (XP_017701989.1), *R. serpentine* (2FP8), *R. verticillata* (AAY81922.1), *N. nimmoniana* (AIL49060.1), *P. somniferum* (AJT49020.1), *M. speciosa* (ADK91432.1), and *D. officinale* (KX068707)

Fig. 5. Phylogenetic tree analysis of DoSTR with STR sequences

Fig. 6. Two sequences alignment of *D. officinale* STR with *N. nimmoniana* STR

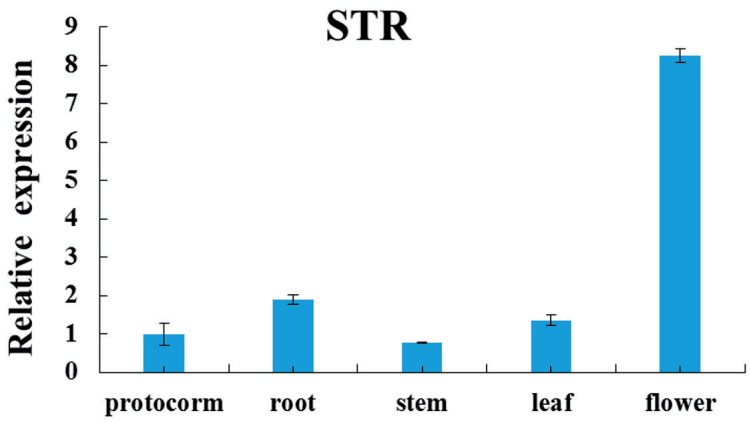

Fig. 7. Gene expression profiles of *DoSTR* in five different tissues

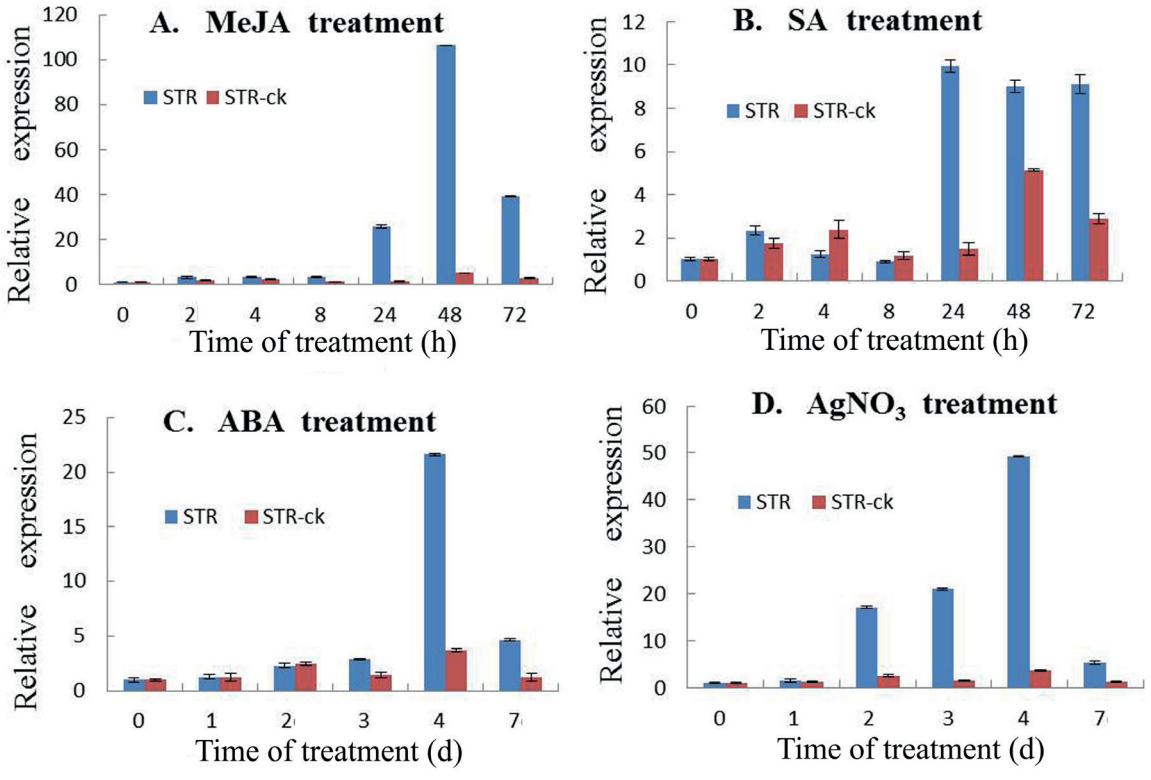

Fig. 8. Relative expression analysis of *DoSTR* treated by three plant growth substances and $AgNO_3$. A, B, C, D are the relative expression analysis of *DoSTR* during MeJA, SA, ABA, $AgNO_3$ treatment and the control for *D. officinale* protocorms, respectively

expression was detected in all the measured organs, including root, stem, leaf, flower and protocorm, although with different expression levels as shown in Figure 7. The relative expression levels of *DoSTR* were the highest in flowers, whereas those were the lowest in stems. In flowers, the expression amounts of *DoSTR* were 10.6 times, 8.3 times, 6.1 times and 4.4 times higher than those in stems, protocorms, leaves and roots, respectively. This result showed that *DoSTR* constitutively expressed in all the tested tissues at different levels, which was the highest in flower, moderate in leaf and root, lowest in stem.

Relative expression analysis of *DoSTR* treated by MeJA, SA, ABA and $AgNO_3$. To analyze the expression characteristics of *DoSTR* in response to biotic and abiotic stimuli, three phytohormones, including MeJA, SA and ABA, together with $AgNO_3$ (as one of the ethylene inhibitors), were applied to treat *D. offcinale* protocorms, respectively. The results showed that the untreated control relative expression of *DoSTR* were in the stable low level at different time, while four different treatments could induce the expression of *DoSTR* with distinct peaks at different treating time (Fig. 8). Under MeJA treatment, the transcript level of *DoSTR* was enhanced by 20.7 times compared to that of the control and reached the highest level at 48h, then decreased at 72h. This expression tendency is accordance with the expression of *HpSTR* [Flores-Sanchez et al. 2016], *CrSTR* [Goklany et al. 2013] and *MsSTR* [Wungsintaweekul et al. 2012] induced by MeJA or JA. SA treatment caused the similar effects on expressions of *DoSTR* with MeJA, but the peak induced by SA was 6.7 times higher than that of the control at 24h and subsequently was decreased slowly. From the A and B of Figure 8, thus it is possibly that the inducing effect on the *DoSTR* expression by SA was less than by MeJA.

The response of *DoSTR* to ABA was relatively slow. Until the third day after treatment, the relative expression of *DoSTR* was only 2 times higher than that of the control. Subsequently the relative expression of *DoSTR*

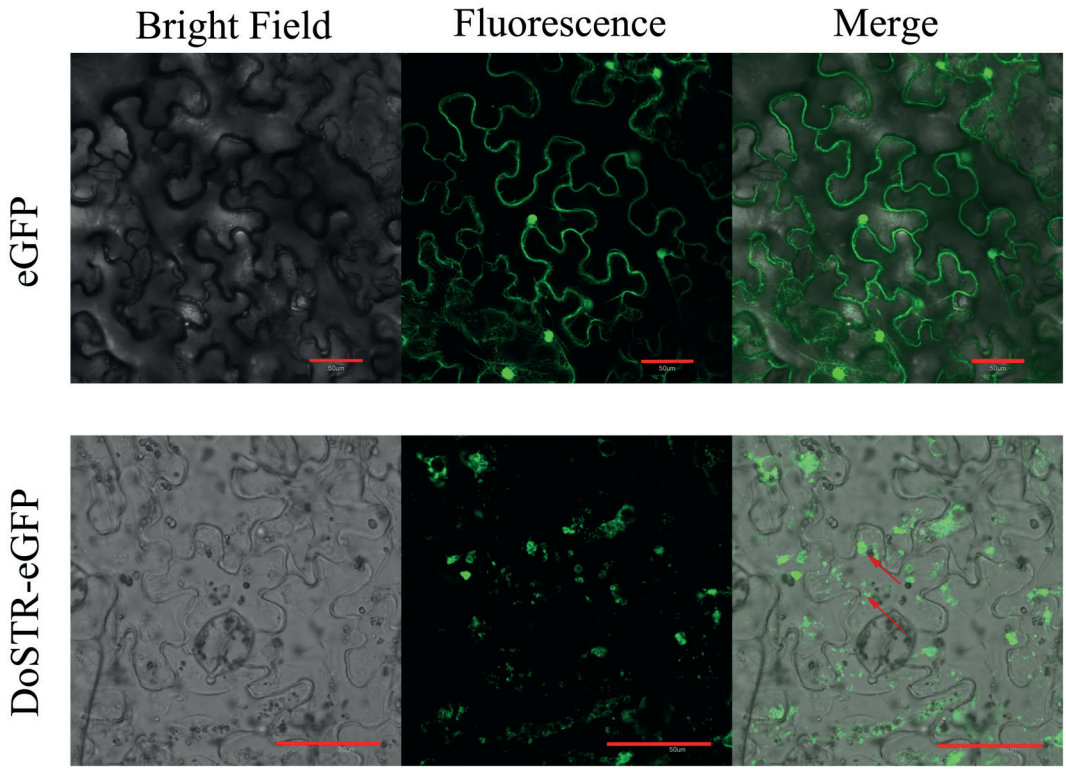

Fig. 9. Subcellular localization analysis of DoSTR. The red arrows showed the site of the DoSTR in tobacco leaves

was sharply raised to 5.8 times compared to that of the control at the fourth day, and decreased at 7d after treatment. Under $AgNO_3$ treatment, the relative expression level of *DoSTR* was elevated from 2d, and peaked at 4d with the expression level 13 times higher than that of the control, subsequently dropped at 7d.

Subcellular localization of *DoSTR*. To determine *DoSTR* subcellular localization patterns, *A. tumefaciens* EHA105 with the fusion expression vector pCambia1301-DoSTR-eGFP was injected into the leaves of tobacco (*N. tabacum*). Compared to the GFP fluorescence which was mainly localized in the nuclei and the cell membrane, the DoSTR-eGFP fluorescence was scatteredly distributed in the whole epidermal cell of tobacco leaf (Fig. 9).

DISCUSSION

D. officinale is an important Chinese medicinal herb and used widely in Asia, Europe and Australia for its diverse tonic components. Among these components, alkaloids were rarely studied comparing with other components for its low concentration, while *D. officinale* produce high-quality alkaloids [Chen et al. 2006]. Therefore researches about alkaloids should be enhanced. Based on the *D. officinale* genome data [Yan et al. 2015], transcriptome data [Guo et al. 2013] and metabolic profiling [Jiao et al. 2018], *D. officinale* alkaloid biosynthetic pathways were enriched in the TIA biosynthesis pathway. Strictosidine synthase was the crucial enzyme in the biosynthetic pathway of TIA [Cui et al. 2015], while the DoSTR was rarely known. In this study, *DoSTR* was first cloned and characterized from *D. officinale*. At the same time, bioinformation analysis, tissue-specific expression, response to different phytohormones and signal molecular and subcellular localization were also tested.

DoSTR cDNA contained a 1179 bp ORF encoding a 392-amino acid protein. BlastP analyses showed that its amino acid sequence was classified into Str_synth superfamily. As shown in Figure 4, both Cys-89 and Cys-101 were highly conserved throughout the Str_synth superfamily. The two Cys residues were considered to be very important for maintaining the integrity of the binding pocket of active STR proteins [Ma 2006]. At the same time, there was a Glu-309 at the active site in DoSTR protein in accordance with RsSTR [Ma 2006]. These results suggested that DoSTR might be an active STR.

From the phylogenetic tree of STRs, STRs from Rubiaceae and Apocynaceae were clustered together, while STRs from monocotyledon plants *Zea mays*, *Elaeis guineensis* and *D. officinale* were clustered together. The phylogenetic relationship of STR is in accordance with the traditional evolutionary classification of plants. As reported, CPT (a kind of TIA) was produced by many species belonged to some unrelated orders within angiosperms [Lorence et al. 2004]. Lorence et al. [2004] supposed that the genes encoding enzymes involved in CPT biosynthesis were evolved early during evolution, and these genes were not lost during evolution but might have been "switched off" during a period of time and "switched on" again at some later. This may explain why many unrelated plants could synthesize TIA.

Tissue expression pattern showed that *DoSTR* constitutively expressed in all the tested tissues at different levels, which was the highest in flower, moderate in leaf and root, lowest in stem. This expression pattern of *DoSTR* is in line with that of *O. japonica STR* [Lu et al. 2009], but is different from that of *R. verticillata STR* [Chen et al. 2008]. Zhang et al. has just reported that the flowers of *D. officinale* are rich in total phenol and flavonoid [Zhang et al. 2019]. Up to now, there are no reports on the content of TIA in different tissue of *D. officinale*. From the tissue expression pattern of *DoSTR*, we guess that the content of TIA is highest of flower, secondly in leaf and root, lowest in stem. And the flowers of *D. officinale* are likely to have important medicinal value.

In this study, MeJA could dramatically induce the transcriptional level of *DoSTR*. It is accordance with the expression of *HpSTR* [Flores-Sanchez et al. 2016], *CrSTR* [Goklany et al. 2013] and *MsSTR* [Wungsintaweekul et al. 2012] induced by MeJA or JA. Because MeJA has been identified as a signaling molecule that could induce gene expression and elicit secondary metabolic pathways in plant cells [Pauwels et al. 2008]. As one of the ethylene inhibitors, $AgNO_3$ effects on the *DoSTR* expression were possibly associated with repressing ethylene pathway. These results suggested that *DoSTR* was expressed at a lower level in untreated protocorms, but it could be induced in response to biotic or abiotic stimuli.

The result of subcellular localization of *DoSTR* showed that the DoSTR-eGFP fluorescence was scatteredly distributed in the whole epidermal cell of tobacco leaf. The vacuole occupies almost whole epidermal cell of tobacco leaf. So we guess the *DoSTR* is mainly localized in the vacuole of tobacco leaf. It suggested that the *DoSTR* could be targeted mainly to the vacuole, which is accordance with the prediction described above and many other *STRs* [Mcknight et al. 1991].

Strictosidine synthase-like proteins are widely existed in multicellular organisms, with the highly diverse functions during the system evolution [Hicks et al. 2011]. Strictosidine synthase-like proteins have been known for roles in animal immune response and in plant defense mechanisms [Kibble et al. 2009]. The bioinformation analysis, tissue-specific expression and subcellular localization of *DoSTR*, all these findings showed that DoSTR were similar with other active STRs and could be classified into Str_synth superfamily. Meanwhile in the metabolic profiling of *D. officinale*, three kinds of TIAs, which are the downstream products of strictosidine, were detected by our group [Jiao et al. 2018]. That is to say there is active STR in *D. officinale*. But strictosidine has not been detected with HPLC in *D. officinale* by our group. Combined with all the results, we speculate that *DoSTR* may well be an active gene and the synthesis of strictosidine is rapidly used to produce downstream products. Next we will measure the activity of DoSTR through genetic transformation and *in vitro* enzyme activity testing. This study may throw light on the alkaloid biosynthesis pathway of *D. officinale*. We believe that with the further research, the TIA metabolic pathway of *D. officinale* will become more and more clear.

ACKNOWLEDGEMENTS

The present investigation is financially supported by Natural Science Foundation of China (31501368, 81573518), Twelfth Five-Year Plan for Science and Technology 19Support of Anhui Province (1301032139), Scientific Research Project of Anhui Provincial Department of Education (KJ2015A005, KJ2018B15, KJ2018A0403, KJ2016A644, KJ2017A846) and The Biology Key Subject Construction of Anhui, Collaborative Innovation Center of Agri-forestry Industry in Dabieshan Area, Anhui Agricultural University.

REFERENCES

Almagro Armenteros, J.J., Tsirigos, K.D., Sønderby, C.K. (2019). SignalP 5.0 improves signal peptide predictions using deep neural networks. Nat. Biotechnol., 37, 420–423. DOI: 10.1038/s41587-019-0036-z

Artimo, P., Jonnalagedda, M., Arnold, K., Baratin, D., Csardi, G., Castro, E. de, Duvaud, S., Flegel, V., Fortier, A., Gasteiger, E., Grosdidier, A., Hernandez, C., Ioannidis, V., Kuznetsov, D., Liechti, R., Moretti, S., Mostaguir, K., Redaschi, N., Rossier, G., Xenarios, I., Stockinger, H. (2012). ExPASy: SIB bioinformatics resource portal. Nucleic Acids Res., 40(W1), W597–W603. DOI: 10.1093/nar/gks400

Benkert, P., Tosatto, S.C.E., Schomburg, D. (2008). QMEAN: A comprehensive scoring function for model quality assessment. Proteins Struct. Funct. Bioinf., 71, 261–277. DOI: 10.1002/prot.21715

Chen, R., Liao, Z.H., Chen, M., Wang, Q., Yang, C.X., Yang, Y.J. (2008). Molecular cloning and characterization of the Strictosidine synthase Gene from *Rauwolfia verticillata*. Russ. J. Plant. Physl., 55, 670–675. DOI: 10.1134/s1021443708050117

Chen, X.M., Xiao, S.Y, Guo, S.X. (2006). Comparison of chemical compositions between *Dendrobium candidum* and *Dendrobium nobile*. Acta. Acad. Med. Sin., 28(4), 524–529. DOI: 10.1360/aps040120

Cui, L., Ni, X., Ji, Q., Teng, X., Yang, Y., Wu, C., Zekria, D., Zhang, D., Kai, G. (2015). Co-overexpression of geraniol-10-hydroxylase and strictosidine synthase improves anti-cancer drug camptothecin accumulation in *Ophiorrhiza pumila*. Sci. Rep., 5, 8227. DOI: 10.1038/srep08227

Flores-Sanchez, I.J., Paniagua-Vega, D., Vera-Reyes, I., Cerda-García-Rojas, C.M., Ramos-Valdivia, A.C. (2016). Alkaloid biosynthesis and metabolic profiling responses to jasmonic acid elicitation in *Hamelia patens* plants by NMR-based metabolomics. Metabolomics, 12, 1–14. DOI: 10.1007/s11306-016-0999-4

Goklany, S., Rizvi, N.F., Loring, R.H., Cram, E.J., Lee-Parsons, C.W.T. (2013). Jasmonate-dependent alkaloid biosynthesis in *Catharanthus roseus* hairy root cultures is correlated with the relative expression of Orca and Zct transcription factors. Biotechnol. Progr., 29, 1367–1376. DOI: 10.1002/btpr.1801

Guo, X., Li, Y., Li, C., Luo, H., Wang, L., Qian, J., Luo, X.,

Xiang, L., Song, J., Sun, C., Xu, H., Yao, H., Chen, S. (2013). Analysis of the *Dendrobium officinale* transcriptome reveals putative alkaloid biosynthetic genes and genetic markers. Gene, 527, 131–138. DOI: 10.1016/j.gene.2013.05.073

He, T., Huang, Y., Yang, L., Liu, T., Gong, W., Wang, X., Sheng, J., Hu, J. (2016). Structural characterization and immunomodulating activity of polysaccharide from *Dendrobium officinale*. Int. J. Biol. Macromol., 83, 34–41. DOI: 10.1016/j.ijbiomac.2015.11.038

Hicks, M.A., Barber, A.E., Giddings, L., Caldwell, J., O'Connor, S.E., Babbitt, P.C. (2011). The evolution of function in strictosidine synthase-like proteins. Proteins Struct. Funct. Bioinf., 79, 3082–3098. DOI: 10.1002/prot.23135

Huang, K.W., Li, Y.R., Tao, S.C., Wei, G., Huang, Y., Chen, D., Wu, C. (2016). Purification, characterization and biological activity of polysaccharides from *Dendrobium officinale*. Molecules, 21, 701. DOI: 10.3390/molecules21060701

Irmler, S., Schroder, G., St-Pierre, B., Crouch, N.P., Hotze, M., Schmidt, J., Strack, D., Matern, U., Schroder, J. (2000). Indole alkaloid biosynthesis in *Catharanthus roseus*: new enzyme activities and identification of cytochrome P450CYP72A1 as secologanin synthase. Plant. J., 24, 797–804. DOI: 10.1111/j.1365-313X.2000.00922.x

Jiao, C.Y., Song, C., Zheng, S.Y., Zhu, Y.P., Jin, Q., Cai, Y.P., Lin, Y. (2018). Metabolic Profiling of *Dendrobium officinale* in Response to Precursors and Methyl Jasmonate. Int. J. Mol. Sci., 19(3), 728–746. DOI: 10.3390/ijms19030728

http://www.cbs.dtu.dk/services/SignalP/

http://www.expasy.org

http://www.ncbi.nlm.nih.gov/orffinder/

https://www.predictprotein.org/

Kibble, N.A.J., Sohani, M.M., Shirley, N., Byrt, C., Roessner, U., Bacic, A., Schmidt, O., Schultz, C.J. (2009). Phylogenetic analysis and functional characterisation of strictosidine synthase-like genes in *Arabidopsis thaliana*. Funct. Plant. Biol., 36, 1098–1109. DOI: 10.1071/FP09104

Kutchan, T.M. (1989). Expression of enzymatically active cloned stritosidine synthase from the higher-plant *Rauvolfia serpentina* in *Escherichia coli*. Febs. Lett., 257, 127–130. DOI: 10.1016/0014-5793(89)81802-2

LopezMeyer, M., Nessler, C.L. (1997). Tryptophan decarboxylase is encoded by two autonomously regulated genes in *Camptotheca acuminata* which are differentially expressed during development and stress. Plant. J., 11, 1167–1175. DOI: 10.1046/j.1365-313X.1997.11061167.x

Lorence, A., Nessler, C.L. (2004). Camptothecin, over four decades of surprising findings. Phytochemistry, 65, 2735–2749. DOI: 10.1016/j.phytochem.2004.09.001

Lu, H., McKnight, T.D. (1999). Tissue-specific expression of the beta-subunit of tryptophan synthase in *Camptotheca acuminata*, an indole alkaloid-producing plant. Plant. Physiol., 120, 43–51. DOI: 10.1104/pp.120.1.43

Lu, Y., Wang, H., Wang, W., Qian, Z., Li, L., Wang, J., Zhou, G., Kai, G. (2009). Molecular characterization and expression analysis of a new cDNA encoding strictosidine synthase from *Ophiorrhiza japonica*. Mol. Biol. Rep., 36, 1845–1852. DOI: 10.1007/s11033-008-9389-y

Luo, Q., Tang, Z., Zhang, X., Zhong, Y., Yao, S., Wang, L., Lin, C., Luo, X. (2016). Chemical properties and antioxidant activity of a water-soluble polysaccharide from *Dendrobium officinale*. Int. J. Biol. Macromol., 89, 219–227. DOI: 10.1016/j.ijbiomac.2016.04.067

Ma, X. Panjikar, S., Koeke, J. (2006). The structure of *Rauvolfia serpentina* strictosidine synthase is a novel six-bladed β-propeller fold in plant proteins. Plant Cell, 18, 907–920. DOI: 10.2307/20076650

Manjunatha, B.L., Singh, H.R., Ravikanth, G., Nataraja, K.N., Shankar, R., Kumar, S., Shaanker, R.U. (2016). Transcriptome analysis of stem wood of *Nothapodytes nimmoniana* (Graham) Mabb. identifies genes associated with biosynthesis of camptothecin, an anti-carcinogenic molecule. J. Biosci., 41, 119–131. DOI: 10.1007/s12038-016-9591-3

Mariani, V., Kiefer, F., Schmidt, T., Haas, J., Schwede, T. (2011). Assessment of template based protein structure predictions in CASP9. Proteins Struct. Funct. Bioinf., 79, 37–58. DOI: 10.1002/prot.23177

Mcknight, T.D., Bergey, D.R., Burnett, R.J., Nessler, C.L. (1991). Expression of enzymatically active and correctly targeted strictosidine synthase in transgenic tobacco plants. Planta, 185, 148–152. DOI: 10.1007/BF00194055

Mcknight, T.D., Roessner, C.A., Devagupta, R., Scott, A.I., Nessler, C.L. (1990). Nucleotide-sequence of a cDNA-encoding the vacuolar protein strictosidine synthase from *Catharanthus roseus*. Nucleic. Acids. Res., 18, 4939. DOI: 10.1093/nar/18.16.4939

Ng, T.B., Liu, J., Wong, J.H., Ye, X., Wing Sze, S.C., Tong, Y., Zhang, K.Y. (2012). Review of research on *Dendrobium*, a prized folk medicine. Appl. Microbiol. Biot., 93, 1795–1803. DOI: 10.1007/s00253-011-3829-7

Pasquali, G., Goddijn, O.J., De, W.A., Verpoorte, R.,

Schilperoort, R.A. (1992). Coordinated regulation of two indole alkaloid biosynthetic genes from *Catharanthus roseus* by auxin and elicitors. Plant. Mol. Biol., 18, 1121–1131. DOI: 10.1007/BF00047715

Pauwels, L., Morreel, K., De Witte, E., Lammertyn, F., Van Montagu, M., Boerjan, W., Inzé, D., Goossens, A. (2008). Mapping methyl jasmonate-mediated transcriptional reprogramming of metabolism and cell cycle progression in cultured *Arabidopsis* cells. PNAS, 105(4), 1380–1385. DOI: 10.1073/pnas.0711203105

Pfaffl, M.W. (2001). A new mathematical model for relative quantification in real-time RT-PCR. Nucleic. Acids. Res., 29, 2002–2009. DOI: 10.1093/nar/29.9.e45

Stevens, L.H., Giroud, C., Pennings, E., Verpoorte, R. (1993). Purification and characterization of strictosidine synthase from a suspension-culture of *Cinchona robusta*. Phytochemistry, 33, 99–106. DOI: 10.1016/0031-9422(93)85403-E

Venditto, V.J., Simanek, E.E. (2010). Cancer therapies utilizing the camptothecins: a review of the *in vivo* literature. Mol. Pharm., 7, 307–349. DOI: 10.1021/mp900243b

Wang, C.T., Liu, H.T., Gao, X.S., Zhang, H. (2010). Overexpression of G10H and ORCA3 in the hairy roots of *Catharanthus roseus* improves catharanthine production. Plant. Cell. Rep., 29, 887–894. DOI: 10.1007/s00299-010-0874-0

Wei, W., Feng, L., Bao, W.R., Ma, D.L., Leung, C.H., Nie, S.P., Han, Q.B. (2016). Structure characterization and immunomodulating effects of polysaccharides isolated from *Dendrobium officinale*. J. Agric. Food. Chem., 64(4), 881–889. DOI: 10.1021/acs.jafc.5b05180

Wheeler, D.L., Barrett, T., Benson, D.A., Bryant, S.H., Canese, K., Chetvernin, V. (2007). Database resources of the national center for biotechnology information. Nucleic Acids Res., 35(Database), D5–D12. DOI: 10.1093/nar/gkl1031

Wungsintaweekul, J., Choo-malee, J., Charoonratana, T., Keawpradub N. (2012). Methyl jasmonate and yeast extract stimulate mitragynine production in *Mitragyna speciosa* (Roxb.) Korth. shoot culture. Biotechnol. Lett., 34, 1945–1950. DOI: 10.1007/s10529-012-0968-6

Xu, J., Han, Q., Li, S., Chen, X., Wang, X., Zhao, Z., Chen, H. (2013). Chemistry, bioactivity and quality control of *Dendrobium*, a commonly used tonic herb in traditional Chinese medicine. Phytochem. Rev., 12, 341–367. DOI: 10.1007/s11101-013-9310-8

Yachdav, G., Kloppmann, E., Kajan, L., Hecht, M., Goldberg, T., Hamp, T., Hönigschmid, P., Schafferhans, A., Roos, M., Bernhofer, M., Richter, L., Ashkenazy, H., Punta, M., Schlessinger, A., Bromberg, Y., Schneider, R., Vriend, G., Sander, Ch., Ben-Tal, N., Rost, B. (2014). PredictProtein – an open resource for online prediction of protein structural and functional features. Nucleic Acids Res., 42(Web Server issue), W337–W343. DOI: 10.1093/nar/gku366

Yamazaki, Y., Sudo, H., Yamazaki, M., Aimi, N., Saito, K. (2003). Camptothecin biosynthetic genes in hairy roots of *Ophiorrhiza pumila*: cloning, characterization and differential expression in tissues and by stress compounds. Plant. Cell. Physiol., 44, 395–403. DOI: 10.1093/pcp/pcg051

Yan, L., Wang, X., Liu, H., Tian, Y., Lian, J., Yang, R., Hao, S., Wang, X., Yang, S., Li, Q., Qi, S., Kui, L., Okpekum, M., Ma, X., Zhang, J., Ding, Z., Zhang, G., Wang, W., Dong, Y., Sheng, J. (2015). The Genome of *Dendrobium officinale* Illuminates the Biology of the Important Traditional Chinese Orchid Herb. Mol. Plant., 8, 922–934. DOI:10.1016/j.molp.2014.12.011

Zhang, X., Zhang, S., Gao, B., Qian, Z., Liu, J., Wu, S., Si, J. (2019). Identification and quantitative analysis of phenolic glycosides with antioxidant activity in methanolic extract of *Dendrobium catenatum* flowers and selection of quality control herb-markers. Food Res. Int., 123, 732–745.

Zhu, N., Han, S., Yang, C., Qu, J., Sun, Z., Liu, W., Zhang, X. (2016). Element-tracing of mineral matters in *Dendrobium officinale* using ICP-MS and multivariate analysis. SpringerPlus, 5, 1–9. DOI: 10.1186/s40064-016-2618-2

Xu, R.X., Cao, F.X., Peng, J.Q., Si, S.B. (2012). Cloning and analysis of strictosidine synthase in *Rauvolfia yunnanensis*. J. Cent. South. Univ. For Technol., 32, 128–131. DOI: 10.1007/s11783-011-0280-z